

# Design and Control of an Agile Robotic Fish With Integrative Biomimetic Mechanisms

Shiwu Zhang, *Member, IEEE*, Yun Qian, Pan Liao, Fenghua Qin, and Jiming Yang

**Abstract**—Flying insects and swimming fishes have high efficiency and high maneuverability in air and water, respectively. Their wings and fins have evolved for many ages to adapt to propelling in the complex environment. In this paper, an integrative biomimetic robotic fish is proposed and developed, which combines the advantages of insect wings and fish fins to achieve a high agility underwater. In the robotic fish, two caudal fins were equipped at the tail of the robotic fish in parallel as the main propulsion mechanism, the opposite flapping of the two caudal fins generates mutually opposing lateral forces during cruising, which leads to a stable and high-performance swimming. In addition, two pectoral fins that mimic the function of insect wings were equipped at two sides of the robotic fish, which enhances the robotic fish maneuverability in vertical plane. Moreover, a central pattern generator model was designed to achieve the versatile maneuvering motions, motion switching, and autonomous swimming with an obstacle avoiding ability. The experiments have demonstrated that the robotic fish can swim more stably and efficiently with versatile maneuvering motions by taking advantage of the integrative propulsion mechanism. The developed robotic fish have many potential applications for its agility, stable swimming, and low-cost structure.

**Index Terms**—Agility, central pattern generator (CPG), integrative biomimetic mechanisms, maneuverability, robotic fish.

## I. INTRODUCTION

DEVELOPING an agile robotic fish capable of overcoming complex underwater environments is expected for the emergent requirements in many areas such as biological study, resource exploration, and disaster rescue. Since the first robotic fish, RoboTuna, was developed in 1995 [1], there have been many robotic fishes that mimic various kinds of fishes in the past years. According to the location of propulsion mechanisms, the propulsion methods of robotic fishes can be classified into two categories [2]: 1) body and/or caudal fins propulsion (BCF) [3]–[5] and 2) middle and/or paired fins propulsion (MPF) [6]–[11].

Manuscript received June 22, 2015; revised October 18, 2015; accepted April 06, 2016. Date of publication April 21, 2016; date of current version August 12, 2016. Recommended by Technical Editor S. Park. This work was supported by the National Natural Science Foundation of China under Grant 51375468.

S. Zhang, Y. Qian, and P. Liao are with the Department of Precision Machinery and Precision Instrumentation, University of Science and Technology of China, Hefei 230026, China (e-mail: swzhang@ustc.edu.cn; qianyun@mail.ustc.edu.cn; lpan@mail.ustc.edu.cn).

F. Qin and J. Yang are with the Department of Modern Mechanics, University of Science and Technology of China, Hefei 230026, China (e-mail: qfh@ustc.edu.cn; jmyang@ustc.edu.cn).

This paper has supplementary downloadable multimedia material available at <http://ieeexplore.ieee.org>.

Color versions of one or more of the figures in this paper are available online at <http://ieeexplore.ieee.org>.

Digital Object Identifier 10.1109/TMECH.2016.2555703

However, the current most robotic fishes are far from duplicating the locomotion characteristics of real fishes, which also sets up an obstacle for their applications in engineering. For example, the locomotion performance, especially the speed of most developed robotic fishes is far lower than that of fishes. Besides swimming speed, the instability arising from the undulation of body and caudal fin also affects the locomotion performance heavily. “Yaw” motion comes from the momentum exerted on the head of fish that compensates the propulsion motion of the tail. The instability impedes the applications such as environment monitoring with the camera. Moreover, the maneuverability of the developed robotic fish is insufficient, especially the maneuvers in vertical plane such as rising and sinking. Inspired by real fishes, robotic fishes usually adopt buoyancy changing by adjusting water displacement or body gesture altering by adjusting center of gravity to achieve maneuvers in vertical plane. However, the methods are not satisfying and lead to a heavy and bulky structure, which also increases complexity of motion controlling. The dolphin robot has developed an excellent agility in vertical plane [12], while the maneuverability in horizontal plane is limited for the less flexibility of body involving movement in maneuvers. The deficiency in motion control of the robotic fishes is another issue that needs more efforts. The stability and maneuverability of fishes not only arise from their unique structures and muscles, but also from the natural control strategy, which ensures the transition of motions is natural and efficient. With the constraints of the limited performance from driving units, such as artificial muscles and motors, to the poor flexibility of the controlling strategy, there is not a biomimetic robot that can compass the whole aforementioned problems.

Fortunately, nature has provided plenty of excellent samples to inspire us in the design of locomotion mechanisms. Moreover, incorporating efficient biomimetic mechanisms inspired by different animals into one biomimetic robot may lead to a considerable performance improvement. Animal usually keeps stable and maneuverable simultaneously, which is hardly duplicated by a biomimetic robot. The secret is that animals may utilize opposing forces exerted by their appendages [13]. For example, knife fishes are found utilizing mutually opposing force during swimming to improve both stability and maneuverability [14]. Cockroach usually utilizes opposite forces exerted by legs on two sides of the body to propel and to keep a stable locomotion [13], [15]. Inspired by the opposite force adopted by animals, we utilize two caudal fins that are arranged in parallel to propel the developed robotic fish. The opposite flapping of two caudal fins will generate opposing lateral forces, which can counteract the yaw motion, and may lead to a stable swimming and a high-speed swimming. Insects possess a remarkable flying ability in the air with the flapping wings. Insects can

take off backwards, flying sideway, hovering aloft, and carrying loads that exceed twice body weight [16]. The great agility of insects, especially for dipteran, arises from the kinematics of the two flapping wings. There have been many efforts to explain the high force produced by two flapping wings and to duplicate the model of the flying insects [17]–[20]. Inspired by the high maneuverability of flying insects, a pair of pectoral fins whose motions are similar to those of insect wings are developed and equipped at both sides of the robotic fish. At an identical Reynolds number, the flapping pectoral fins may also endow the robotics fish a high maneuverability in vertical plane.

The high-performance swimming and flying of animals arises not only from the interactional forces by their unique locomotory appendages, but also from the coordinated interaction between the mechanisms and the control system, called central pattern generator (CPG). A CPG can produce rhythmic oscillations that can be utilized to control the rhythmic motion of animals appendages, such as fish fins, insect wings, and animal limbs [21]. Recently, the rhythmic motions strategy generated by the CPG have been applied in the control of biomimetic and bioinspired underwater robots to improve their locomotion performance [8], [22]–[24]. From biology viewpoint, The CPG is very suitable for the control of a robotic fish.

- 1) It is very natural to exert a rhythmic movement to control the motion of the joints of the robotic fish.
- 2) The smooth transition of various rhythmic movements provides a potential basis to improve the locomotion performance and the maneuverability of the robotic fish.

To sum up, developing an agile robotic fish needs an aggregation of innovations in locomotory mechanisms and controlling strategy. In this paper, we deliver an interesting attempt to design and control an integrative biomimetic robotic fish that successfully demonstrates agile swimming behaviors. The robotic fish combines the characteristics and mechanisms of insect flying and fish swimming. A dual caudal-fin propulsion mechanism that transcends nature was proposed to improve the locomotory performance and swimming stability. Two wing-like pectoral fins were equipped to provide maneuvering forces in vertical plane. A suitable CPG model was designed to control swimming motions and their smooth switches. Underwater experiments on the robot revealed that the robot possesses a high swimming performance and a high maneuverability, which enables the robot applicable in exploring and performing tasks in a complex underwater environment. Furthermore, the developed robotic fish is very simple, low cost, and modularized, which also increases the possibility of the potential applications.

The remainder of this paper is organized as follows. The detailed design of the composite robotic fish is first described. The structure and the driven module are presented in Section II. The design of the CPG model that adapted to the robotic fish is presented in Section III. In Section IV, the swimming maneuvers of the robotic fish are described. Section V presents the experimental results of the robotic fish, the swimming performance are experimentally analyzed. The advantages of the developed integrative biomimetic robotic fish are also discussed, and the comparison between the robotic fish and other robotic fishes is presented. Finally, concluding remarks are provided in Section VI.

## II. INTEGRATIVE BIOMIMETIC ROBOTIC FISH

The design concept of the developed robotic fish derives from the bionic understanding on the creatures such as fishes and insects. Fish has a high swimming maneuverability and a high swimming propulsion efficiency for its body and fins coordinately movements, while insect has also a high maneuverability with its wings' 3D motions. Integrative biomimetic propulsion mechanism, which combines the advantages of insect and fish propelling mechanisms, will benefit the propulsion performance underwater greatly. The detailed design of integrative biomimetic propulsion mechanism and the structure of the robotic fish are presented later.

### A. Dual-Caudal Fin

Fins play an important role in fish locomotion and maneuverability, such as thrust generating, lateral forces generating for turning, lift forces for hovering, and stability keeping, etc. For example, the caudal fin in BCF mode is the main propeller, while pectoral fins maneuver with other fins [25], [26]. With the coordinated motion of caudal fin and multidegrees-of-freedom body, some BCF-like robotic fishes also achieved a good locomotion performance. For example, G9 series robotic fishes possessed a high maneuverability and a verisimilar swimming [5]; robotic dolphin can jump out of the water recently [12]. Most BCF-like robotic fishes utilized the undulation of body and caudal fin to generate propulsion force. However, there still exists some problems in the current robotic fishes.

- 1) Swimming speed of the robotic fish (often expressed by ratio of swimming speed to body length, usually lower than 1.5 BL/s) was usually much lower than that of real fishes. The cruising of a tuna is about 10 BL/s, while it can reach 20 BL/s in sprinting [27].
- 2) The unstable swimming: "yaw" motion of the robotic fish is much larger than that of the real fish.

The reasons arises from the limited performance of driving motors compared to muscles, in addition to the limited joints of robotic fish body due to the simplicity of the designing structures. Recently, isplash-I has been developed and its remarkable swimming speed reaches 3.4 BL/s [28]. The secret of the success lies in that the robotic fish's unique structure guarantees strict coordinated motion of body joints and caudal fin, which eliminates the kinematic error of the swimming motion due to the limitation of driving motors. However, the unique structure limits isplash-I's maneuverability such as turning and pitching.

Inspired by the fact that mutually opposing forces can improve the stability and maneuverability of the locomotion, a dual-caudal-fin mechanism is proposed for the developed robotic fish to provide the propulsion force. As illustrated in Fig. 1(b), two caudal fins are equipped paralleled at the tail of the robotic fish. When fish swimming forward, the two caudal fins oscillate in an opposite direction (with a phase difference, 180°), and the mutually opposing lateral forces generated by the two caudal fins can effectively improve swimming stability, that decreases the "yaw" motion during swimming. In addition, the opposite flapping motion of the dual-caudal fin is also loosely analogous with jet propulsion, which may lead to a higher swimming

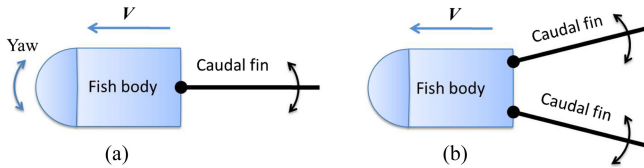


Fig. 1. Schematic diagram of robotic fish propelled by caudal fin. (a) Single caudal fin propulsion. (b) Dual caudal fins propulsion.

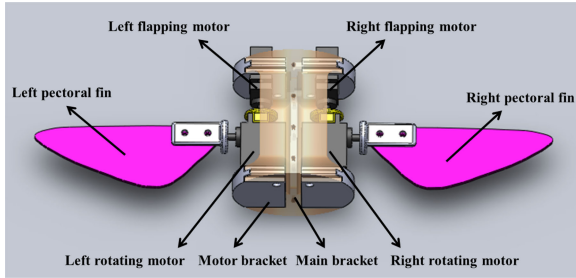


Fig. 2. Module of wing-like pectoral fins. Each pectoral fin has two DOF motions: flapping and rotating. The supportive structure of the driving motor is manufactured by a 3D printing.

performance. In the design, two servo motors (HiTech, HS-5646WP) for the caudal fins are waterproof, with a maximum output torque of 12.9 kg·cm. The shape of the caudal fin is design to match that of Flounder to emphasize the acceleration ability of the robotic fish [27].

### B. Wing-Like Pectoral Fin

Insects have remarkable agility thanks to their flapping wings. The flight with dual-flapping wings, such as flight of flies, has been studied to an intensive extent [17], [29], [30]. The kinematics of the wings can be described by three rotational movements [29], [30]. Along with the understand of the insect flying, many biomimetic flying robots have been developed, which includes scaled models [17], [29] and at-scale models [20], [31]. With a high flapping frequency and a large amplitude, these flying robots also possess a great agility aloft.

In order to explore the aerodynamics of the flapping wings, some studies utilized scaled models flapping in fluid at a similar Reynolds number [29]. Inspired by the agility brought by flapping wings, we designed two insect wing-like pectoral fins for the robotic fish to improve the swimming agility. Insect wings possess a three degree-of-freedom (DOF) wing motion that consists of a wing stroke, a rotation about longitudinal wing axis, and stroke plane deviation. However, the stroke plane deviation usually is small and can be ignored, which simplifies the design of the robotic fly [31]. Thus, the motion of each wing can be simplified into two-DOF movement including stroking and rotating. In our work, we also adopt an analogical two-DOF movement that includes flapping and rotating. Note that the frequency of the wing-like fins underwater is much lower than that of the flies, which is about 1~2 Hz as fishes adopt. The shape of the pectoral fin is designed to match the aspect ratio and area distribution of hoverfly's wing [20], [31].

Fig. 2 displays the module of the wing-like pectoral fins. Every two servo motors that account for a wing-like pectoral

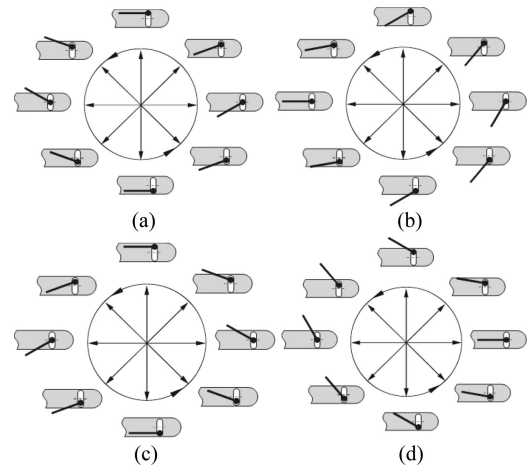


Fig. 3. Typical motion patterns of right pectoral fin. Time moves in a counter-clockwise direction. (a) Forward swimming. (b) Backward swimming. (c) Rising. (d) Sinking.

fin are equipped in one motor bracket, and two motor brackets for left and right pectoral fins are installed in main bracket. The servo motors for the pectoral fins are different from those of caudal fin because they need not output torque as large as that of motors for caudal fins. Here, HS5086WP motors with a 3.6-kg·cm output torque are adopted to propel pectoral fins. Motor brackets and main bracket are manufactured by 3D printing, which saves space and decreases the weight of the robot.

The coordinated movements of the flapping and rotating motion can provide plenty of forces to maneuver the robotic fish. Fig. 3 shows four typical motion patterns of right pectoral fins: that is, forward swimming, backward swimming, rising, and sinking. Being analogical with insect wing motions, flapping (including downstroke phase and upstroke phase) of the pectoral fins is the basic motion, while rotating motion keeps adjusting the attack angle of the fins during flapping, and in consequence of the magnitude and direction of the instantaneous forces [29]. For example, in order to realize a forward swimming, the right pectoral fin will continue performing flapping motion, while during the transition between downstroke and upstroke, the fin will rotate to guarantee a forward component of the force during swimming. Thus, direction of the mean force during a stroke is forward. With the coordinated motions of the two pectoral fins, plenty of maneuvering patterns such as backward swimming, rising, and sinking can also be realized.

### C. Prototype of the Robotic Fish

The structure of the bioinspired robotic fish is shown in Fig. 4. On the head of the fish, there are three infrared sensors (Sharp GP2Y0A21YK) that can detect the obstacle ahead underwater. Controlling circuit and battery are sealed in a cylindrical can that is arranged at the middle part of the robot, which guarantees the reliability of waterproof. The fish body is made of a PVC tube with a stiffness shell, while the head of the body is made by 3D printing with three windows for the IR sensors. As for the controlling unit, a PIC18F4550 microprocessor is adopted to receive the sensor signals, to solve nonlinear equations of CPGs and to output controlling signals to servo motors. The structure

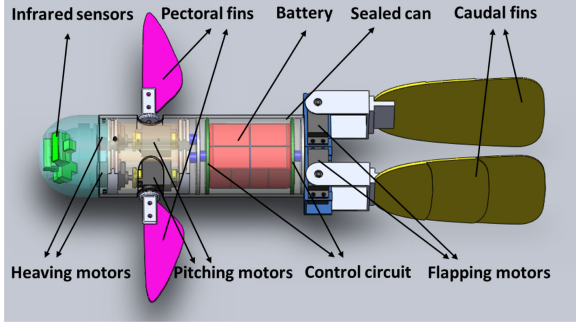


Fig. 4. Schematic diagram of the developed integrative biomimetic robot.

TABLE I  
ROBOTIC FISH SPECIFICATIONS

Parameters	Specifications
Dimensions of robot	440 mm(L) × 80 mm(H) × 316 mm(W)
Weight	1.3 kg
Surface area of pectoral fin	29.50 cm <sup>2</sup> ;
Dimensions of pectoral fin	Wingspan: 109 mm; Aspect ratio: 4.03
Surface area of caudal fin	240 cm <sup>2</sup> ;
Dimensions of caudal fin	Wingspan: 136 mm; Aspect ratio: 0.77
Maximum speed	1.21 BL/s
Power source	11.1V 2000mAh Li-ion Battery

of the robotic fish is very simple and the cost is also very low. The key specifications of the robotic fish are listed in Table I.

### III. CPG MODEL FOR SWIMMING GAITS OF THE ROBOTIC FISH

Despite the innovation in the structural design of robotic fish, the controlling algorithm for motions of various fins is also the key to realize the agility of the robotic fish. As stated by the biological study, the motions of fins and wings can be described by rhythmic movements. Rhythmic movements are usually employed in motions of creatures that include fishes, animals, birds, and insects. Limbs, fins, and wings can be controlled by the coordinated oscillation signals generated by the vertebration. The coordinated oscillation signals can be modeled by nonlinear oscillators to control the movements of biomimetic robots [32], [33], which include swimming gait generation of robotic manta [8], amphibious robot [22], [24], [34], and other types of fish robots [23], [35]. In order to develop a simple, durable, and low-cost robotic fish with a higher agility and maneuverability. The developed CPG model should satisfy several requirements.

- 1) The nonlinear equations should be simple to decrease the computing cost for the low-cost microprocessor.
- 2) The definition of frequency, amplitude, and the phase difference of the out signals should be clear so the transition of controlling signals is easy to acquire.
- 3) The CPG network can receive the feedback signals from IR sensors to achieve an autonomous swimming.

The development of the CPG network will be described in the following sections.

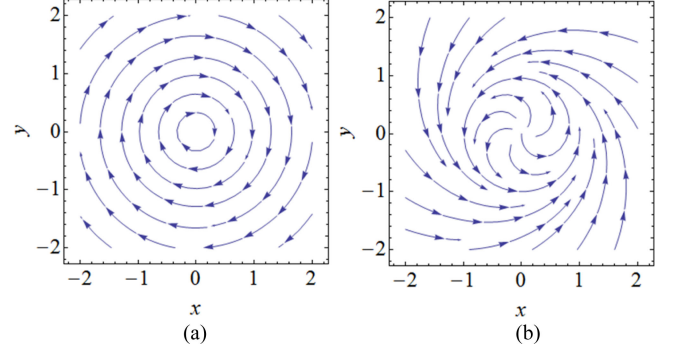


Fig. 5. Phase space of the linear autonomous system. (a) Original oscillator: System is limited in different concentric circles. (b) Revised oscillator: System starts from different initial states, while they all converge into a circle with a certain amplitude (note that,  $r = 0$  is a strange point).

#### A. Generation of Harmonic Oscillator

The rhythmic movement of each joint of the robot can be simplified into a harmonic oscillation. Thus, the first step of modeling the controlling system is to develop a mathematical model that can generate harmonic oscillations. Here, we assume that  $\vec{r}_i = (x_i, y_i)^T$ , where  $\vec{r}_i$  represents the state vectors of two neurons:  $x_i$  and  $y_i$ . For simplicity and low computation cost, a simple linear differential equation is used to describe the neurons

$$\begin{cases} \dot{x}_i = -\omega_i \cdot y_i \\ \dot{y}_i = \omega_i \cdot x_i \end{cases} \quad (1)$$

where  $\omega_i$  denotes the angular frequency of the  $i$ th system, and  $\omega_i = 2\pi f_i > 0, \omega_i \in R, i = 1, 2, \dots, n$ . The system can also be expressed in polar coordinate

$$\dot{\vec{r}} = \begin{bmatrix} \dot{x}_i \\ \dot{y}_i \end{bmatrix} = \begin{bmatrix} 0 & -2\pi f_i \\ 2\pi f_i & 0 \end{bmatrix} \cdot \begin{bmatrix} x_i \\ y_i \end{bmatrix}. \quad (2)$$

The solution of the aforementioned equation is listed as

$$\begin{cases} \dot{x}_i = \dot{r}_i \cos \theta_i - \dot{\theta}_i r_i \sin \theta_i = \frac{\dot{r}_i}{r_i} x_i - \dot{\theta}_i y_i \\ \dot{y}_i = \dot{r}_i \sin \theta_i + \dot{\theta}_i r_i \cos \theta_i = \frac{\dot{r}_i}{r_i} y_i + \dot{\theta}_i x_i \end{cases} \quad (3)$$

where  $\dot{r}_i/r_i = 0$  and  $\theta$  denotes the phase of the oscillator. The solution indicates that the outputs of the neurons are harmonic oscillations with a fixed amplitude. The limited cycle of the autonomous system in phase plane is shown in Fig. 5(a).

In order to modulate the amplitude of the oscillation signals, the differential part:  $\dot{r}/r$  should be revised. The objective of the revision is  $\lim_{t \rightarrow \infty} r_i = R_i$ . Here,  $R_i$  represents the objective amplitude. The rules to modulate the amplitude are listed as follows.

- 1) If  $r_i = R_i$ , then  $\dot{r}_i/r_i = 0$ , system locates equilibrium point.
- 2) If  $r_i < R_i$ , then  $\dot{r}_i/r_i > 0$ , system approaches equilibrium point.
- 3) If  $r_i > R_i$ , then  $\dot{r}_i/r_i < 0$ , system approaches equilibrium point.

Then, a function  $h_{(r_i, R_i, \tau_i)}$  that can meet the aforementioned constraints is defined as follows:

$$\frac{\dot{r}_i}{r_i} = h_{(r_i, R_i, \tau_i)} = \frac{\tau_i(R_i - r_i)}{r_i} \quad (4)$$

where  $\tau_i > 0 (i = 1, 2, 3, \dots, n)$  denotes the parameter that controls the converge speed. Thus, the revised oscillator can be expressed by the following equations:

$$\begin{bmatrix} \dot{x}_i \\ \dot{y}_i \end{bmatrix} = \begin{bmatrix} \frac{\tau_i(R_i - r_i)}{r_i} & -\dot{\theta}_i \\ \dot{\theta}_i & \frac{\tau_i(R_i - r_i)}{r_i} \end{bmatrix} \cdot \begin{bmatrix} x_i \\ y_i \end{bmatrix}. \quad (5)$$

The phase portraits of the revised oscillator is presented in Fig. 5(b). From the figure, we can obtain that the system converges with a certain amplitude. With the aforementioned definition, the rhythmic movements of the joints can be achieved, and the amplitude and the frequency could also be modulated.

### B. Coordination of Two Oscillators

In order to coordinately control the motion of different fins, two oscillators with an adjustable phase difference should also be incorporated in the system. Assuming that  $f_i$  and  $f_j$  are frequency of oscillators  $i$  and  $j$ , respectively, and  $f_i = f_j$ . We set the phase's differential function as  $\dot{\theta}_i = 2\pi f_i + q_i$ ,  $q_i$  denotes the coupled part that controls the phase difference between two oscillators. Then, the dynamic of two oscillators can be expressed as follows:

$$\begin{bmatrix} \dot{x}_i \\ \dot{y}_i \\ \dot{x}_j \\ \dot{y}_j \end{bmatrix} = \begin{bmatrix} 0 & -2\pi f_i & 0 & 0 \\ 2\pi f_i & 0 & 0 & 0 \\ 0 & 0 & 0 & -2\pi f_j \\ 0 & 0 & 2\pi f_j & 0 \end{bmatrix} \cdot \begin{bmatrix} x_i \\ y_i \\ x_j \\ y_j \end{bmatrix} + \begin{bmatrix} \frac{\dot{r}_i}{r_i} & -q_i & 0 & 0 \\ q_i & \frac{\dot{r}_i}{r_i} & 0 & 0 \\ 0 & 0 & \frac{\dot{r}_j}{r_j} & -q_j \\ 0 & 0 & q_j & \frac{\dot{r}_j}{r_j} \end{bmatrix} \cdot \begin{bmatrix} x_i \\ y_i \\ x_j \\ y_j \end{bmatrix} \quad (6)$$

where  $x_j$  and  $y_j$  denote the state of two neurons of oscillator  $j$ , respectively. Similar to the previous rules about amplitude adjusting, we can obtain the following rules for phase adjusting.

- 1) If  $\theta_i - \theta_j = \phi_{ij} + 2k\pi, k \in \mathbb{Z}$ , then  $\dot{\theta}_i = 2\pi f_i; q_i = 0$ , system locates equilibrium point, the system becomes a linear system.
- 2) If  $\theta_i - \theta_j < \phi_{ij} + 2k\pi, k \in \mathbb{Z}$ , then  $\dot{\theta}_i > 2\pi f_i; \dot{\theta}_j < 2\pi f_j; q_i > 0$ , system approaches equilibrium point.
- 3) If  $\theta_i - \theta_j > \phi_{ij} + 2k\pi, k \in \mathbb{Z}$ , then  $\dot{\theta}_i < 2\pi f_i; \dot{\theta}_j > 2\pi f_j; q_i < 0$ , system approaches equilibrium point.

In the aforementioned rules,  $\phi_{ij}$  denotes the objective phase difference between the two oscillators. According to the aforementioned rules, the coupling function can be constructed as

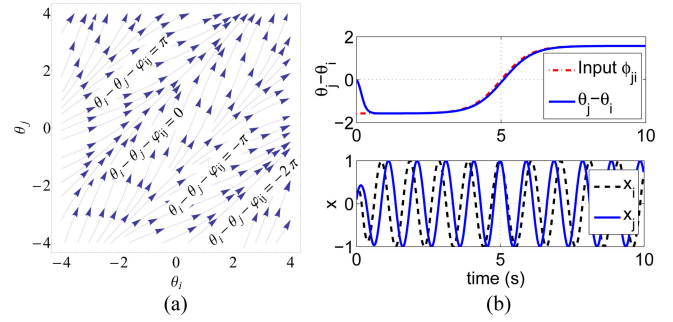


Fig. 6. Two coupled oscillators: (a) dynamics of phase difference; and (b) example of the phase difference adjusting. Initial value of  $r_i, r_j$  are all set as 0.  $\phi_{ij} = \pi/2 + \pi \tanh(t - 5)$ .

follows:

$$\tilde{q}_i = -y_i(x_j \cos \phi_{ij} - y_j \sin \phi_{ij}) + (x_j \sin \phi_{ij} + y_j \cos \phi_{ij}). \quad (7)$$

Thus, the coupled oscillators  $i$  and  $j$  can be expressed by the following equations:

$$\begin{bmatrix} \dot{r}_i \\ r_i \\ \dot{\theta}_i \end{bmatrix} = \begin{bmatrix} \frac{\tau_i(R_i - r_i)}{r_i} \\ \omega_i - r_i r_j \sin(\theta_i - \theta_j - \phi_{ij}) \end{bmatrix} \quad (8)$$

and

$$\begin{bmatrix} \dot{r}_j \\ r_j \\ \dot{\theta}_j \end{bmatrix} = \begin{bmatrix} \frac{\tau_j(R_j - r_j)}{r_j} \\ \omega_j - r_j r_i \sin(\theta_i - \theta_j - \phi_{ij}) \end{bmatrix}. \quad (9)$$

However, in the aforementioned equations,  $\theta_i - \theta_j - \phi_{ij} = (2k + 1)\pi, (k \in \mathbb{Z})$  also can lead to  $\sin(\theta_i - \theta_j - \phi_{ij}) = 0$ , which is a redundant equilibrium point. In order to investigate the stability of the equilibrium point, we assume that  $\omega_i = \omega_j = 2\pi$ ,  $R_i = R_j = 1$ , and  $\theta_{ji} = \pi$ , and plot the dynamics of phase difference between two oscillators in Fig. 6(a). From the figure, we could obtain that the equilibrium points  $\theta_i - \theta_j - \phi_{ij} = (2k + 1)\pi, (k \in \mathbb{Z})$  are unstable. A small disturbance will cause the system converge into objective equilibrium points. Fig. 6(b) delivers an example of the dynamics of system with a phase difference adjusting at time 5. It can be concluded that the converging speed of the system is relative high.

### C. Design of a CPG Network

After constructing two coupled oscillators, we could extend the coupling relationship to any number of oscillators and construct a neural network with a typical topology. Fig. 7 illustrates the coupled relationship of oscillator  $i$  with other oscillators. The following equation describes the oscillator in polar coordination:

$$\begin{bmatrix} \dot{r}_i \\ r_i \\ \dot{\theta}_i \end{bmatrix} = \begin{bmatrix} \frac{\tau_i(R_i - r_i)}{r_i} \\ \omega_i + r_i \sum_{j \neq i}^n w_{ij} r_j \sin(\theta_i - \theta_j - \phi_{ij}) \end{bmatrix} \quad (10)$$

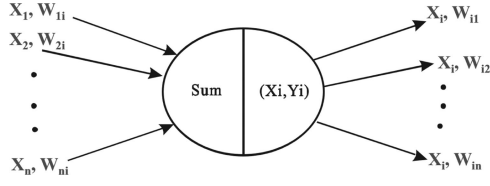


**Fig. 7.** Illustration of the neural network that displays the coupled relationship of oscillators.  $x_i$  and  $y_i$  denote the internal state of oscillator  $i$ , while  $w_{ij}$  denote the weight that oscillator  $i$  to oscillator  $j$ .

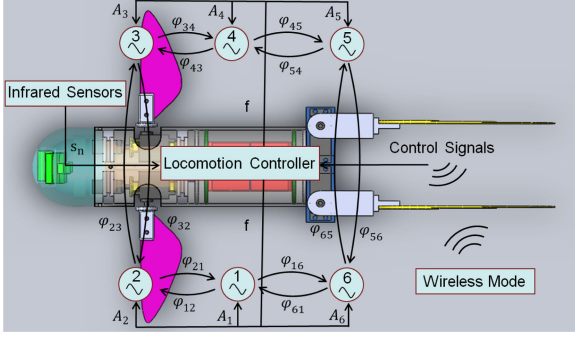


**Fig. 8.** Illustration of the CPG network utilized to control the robotic fish.

where  $w_{ij}$  denotes the weight between oscillator  $i$  and oscillator  $j$ .  $w_{ij} = 0$  means that there is no connection between oscillators  $i$  and  $j$ . With aforementioned definition, a CPG network that control the joints of the integrative biomimetic robotic fish will be constructed, which is illustrated in Fig. 8. Six oscillators are connected into a circle and utilized to control the motion of the robotic fish. Neuron  $x$  in the oscillator are sent to control the servo motor. Specifically, oscillators 1 and 2 output the controlling signal for the flapping and rolling motors of left pectoral fin, while oscillators 3 and 4 are responsible for the rolling and flapping motors of right pectoral fin, and oscillators 5 and 6 control the oscillation of left and right caudal fins, respectively. A PIC18F4550 microprocessor is responsible for determining the amplitude, frequency, and phase difference among various oscillators, and calculating the angular data for the motors according to the oscillating equations.

For the realization of maneuverability of the robotic fish, left pectoral fin, right pectoral fin, and the two caudal fins should coordinately oscillate, thus the topology of the CPG network determines the phase controlling matrix as follows:

$$\phi = \begin{bmatrix} 0 & -\phi_{21} & \cdots & \cdots & 0 & \phi_{16} \\ \phi_{21} & 0 & -\phi_{32} & \cdots & 0 & 0 \\ \vdots & \phi_{32} & 0 & -\phi_{43} & \cdots & \vdots \\ \vdots & \vdots & \phi_{43} & 0 & -\phi_{54} & \vdots \\ 0 & 0 & \vdots & \phi_{54} & 0 & 0 \\ -\phi_{16} & 0 & \cdot & \cdot & 0 & 0 \end{bmatrix}. \quad (11)$$

In order to achieve a close loop, we define that  $\phi_{21} + \phi_{32} + \phi_{43} + \phi_{54} + \phi_{16} = 2k\pi$  ( $k \in \mathbb{Z}$ ). In the equation,  $\phi_{ij}$  is defined as an arctan function, which leads the dynamical system into a

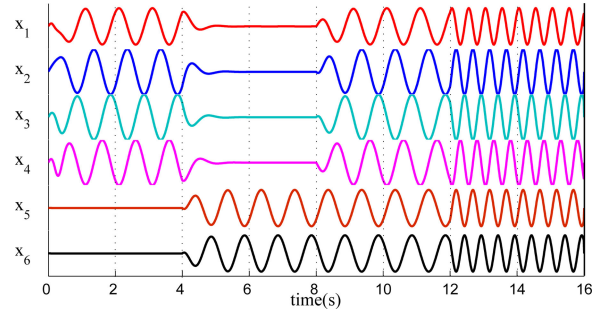


**Fig. 9.** Simulation of cruising with various fins. (0–4) s: cruising with two pectoral fins, two caudal fins nearly keep still. (4–8) s: cruising with two caudal fins, oscillation amplitude of the two pectoral fins are nearly zero. (8–12) s: cruising with four fins. (12–16) s: cruising with four fins at a higher frequency and larger oscillation amplitude, which may lead to a high cruising speed.

stable equilibrium state and avoid to be tracked into an unstable isolated singular point.

#### IV. SWIMMING WITH THE CPG NETWORK

With the two paralleled caudal fins and two wing-like pectoral fins, the developed robotic fish possesses a high maneuverability. The pectoral fins can act as vectored thruster, and the coordinately motions of the four fins enforce the robotic fish multi-DOF movements such as steady cruising, backward swimming, rising, sinking, turning, and rolling. With the information from the three infrared sensors at the head of the robotic fish, it can perform an autonomous swimming with obstacle avoiding ability underwater, which is useful for the autonomous locomotion in complex underwater environment.

##### A. Cruising

Thanks to the various fins, the robotic fish could realize a cruising motion with various methods. For example, the robotic fish may utilize its pectoral fins to flap and roll, utilize its caudal fins to oscillate in opposite direction, or utilize its four fins' coordinate movement to exert a forward thrust. The simulation of the cruising with various fins is presented in Fig. 9. The cruising motion involves four stages, which correspond to swimming with pectoral fins, swimming with caudal fins, swimming with four fins, and swimming with a higher frequency and a larger amplitude, respectively. The simulation signal indicates that the transition between cruising motion with various vectored fins are very smooth, which also benefits a higher locomotory performance.

Despite cruising with various fins, another merit of the robotic fish is its stable and efficient swimming with the caudal fins opposite flapping. It can be achieved by just adjusting the phase difference between oscillator 5 and oscillator 6,  $\phi_{56}$ , from 0 to  $\pi$ .

##### B. Maneuvers

According to the previous analysis, the maneuvers of the robotic fish depend on the coordinately oscillation of six motors. There are three kinds of controlling parameters for the

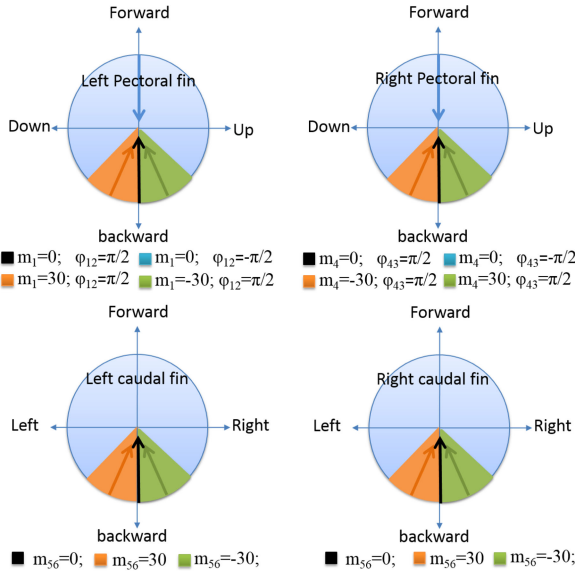


Fig. 10. Illustration of vectored thrust of the four fins. Pectoral fins could vary their thrust direction in vertical plane, while caudal fin could vary their thrust direction in horizontal plane. Various coordinately motions of fins will lead to a high maneuverability of the robotic fish. (Note that,  $R_i$  will be set as a relative small value if motor  $i$  need keep still.)

controlling of maneuvers of the robot: phase difference  $\phi$ , amplitude  $R$ , and oscillation bias  $m$ . The two pectoral fins could alter their thrust direction in vertical planes, while the two caudal fins could alter them in horizontal plane. Fig. 10 illustrates the relationship between the controlling parameters and the vectored thrust of the pectoral fins and the caudal fins.

The combination of the four vectored thrust that exerted by the fins enables the robotic fish a multi-DOF maneuverability underwater. For example, backward swimming by pectoral fins request the two pectoral fins exerting backward thrust and the two caudal fins keeping still. Rising motion involves two pectoral fins' up thrust, while rolling motion requires the opposite thrust that the two pectoral fins output.

### C. Switching Maneuvers

One remarkable advantage of the CPG controlling strategy is the smooth changing of the output signal's parameters, such as the amplitude, frequency, and phase difference. Thanks to the advantage, the smooth transition among various maneuvers can be realized with the combining change of the parameters, which has been validated by the study on the motion of animals and robots [22], [32]. There are many parameters to control the maneuvers of the robotic fish. Here, we adopt an arc tangent function to switch the parameters and achieve a smooth maneuvers switching. Fig. 11 displays the simulation of some maneuvers switching. In the simulation, the robotic fish performs many maneuvers such as cruising, rising, rolling, sinking and backward swimming swims, and the switch among them.

### D. Autonomous Swimming

In order to achieve an autonomous swimming, we equipped three infrared sensors accounting for the detection of obstacles

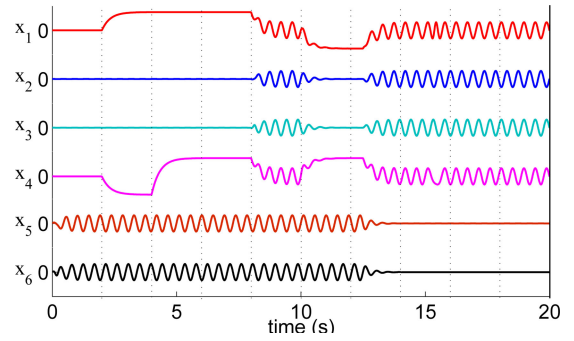


Fig. 11. Simulation of switching maneuvers: (0–2) s: cruising with caudal fins; (2–4) s: rising with two pectoral fins, two caudal fins still provide propulsion forces; (4–8) : rolling with the two pectoral fins; (8–10) s: cruising with four fins; (10–12.5) s: sinking with two pectoral fins, two caudal fins still provide propulsion forces; (12.5–15) s: cruising with pectoral fins, caudal fins keeping still; (15–20) s: swimming backward.

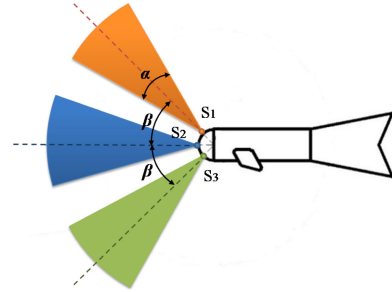


Fig. 12. Illustration of autonomous swimming with the infrared sensors.  $S_1$ ,  $S_2$ , and  $S_3$  represent the area that the upper infrared sensor, the middle infrared sensor, and the lower infrared sensor can detect, respectively. The inclined angle,  $\beta$ , for the upper and lower sensor is  $45^\circ$ , and the detect angle  $\alpha$  is  $40^\circ$ . The detected distance of sensor  $i$ ,  $s_i$ , can be adjusted in advance.

TABLE II  
RELATIONSHIP BETWEEN SENSORS INFORMATION AND MANEUVERS

$s_1$	$s_2$	$s_3$	Maneuvers
X	0	X	Cruising
0	1	X	Rising and cruising
1	1	0	Sinking and cruising
1	1	1	Backward swimming

Note: "0" denotes there is no obstacle detected, "1" denotes there is obstacle ahead, while "X" denotes double cases.

ahead. Three infrared sensors are arranged vertically on the head of the robotics fish. There is an inclined angle for the upper and lower sensors, respectively, which enables the two sensors detect the obstacles from different directions. Fig. 12 illustrates the detect area of the three infrared sensors on the robotic fish. With the information from the three infrared sensors as the feedback of the CPG network, the robot could change gaits or maneuvers to avoid the obstacle and realize an autonomous swimming.

Table II lists the relationship between the sensors' feedback and the corresponding maneuvers that the robotic fish will perform in vertical plane. It should be noticed that if the middle sensor detects an obstacle while the upper sensor does not, the

robotic fish will swim upward despite the result of the lower sensor. The reason lies that the fish incline to avoids to touch the obstacles on the bottom of water.

According to the relationship in Table II, the controlling function for the parameters can be deduced and presented as follows:

$$\left\{ \begin{array}{l} R_5 = R_6 = R - (1 + \tanh(t_2 - s_2))((1 + \tanh(t_1 - s_1)) \\ \quad (1 + \tanh(t_3 - s_3))R/8) + \epsilon \\ m_1 = -m_4 = M(1 + \tanh(t_2 - s_2))((1 - \tanh(s_1 - t_1)) \\ \quad (\tanh(s_3 - t_3) + 3) - 4)/8 \\ \phi_{21} = \phi_{34} = (1 + \tanh(t_2 - s_2))(1 + \tanh(t_1 - s_1)) \\ \quad (1 + \tanh(t_3 - s_3))\pi/8 - \pi/2 \end{array} \right. \quad (12)$$

where  $R$  and  $M$  represent the referred amplitude and bias, respectively.  $t_i$  denotes the threshold setting for sensor  $i$ ,  $s_i$  denotes the information return by sensor  $i$ . A small value  $\epsilon$  setting as 0.01 is utilized to avoid the amplitude equals to zero and to keep the system stable.

## V. EXPERIMENTAL RESULTS

With the integrative biomimetic design on the pectoral fins and caudal fins, the robotic fish propelled by multiple vector thrusters has been developed. Combining the natural rhythm motions generator—CPG network, the robotic fish can realize plenty of maneuvers in a complex underwater environment. A large number of experiments were conducted to validate the model and the controlling strategy. Before the experiment on the robotic fish, the underwater calibration of the servo motors' driving ability was conducted to ensure the amplitude and frequency of the robotic fins driven by servomotors. The experiments were conducted in a rectangular tank with size 5000 mm × 500 mm × 600 mm (length × width × height). A high-speed camera was equipped in a translational slide to track and record the side-view swimming motion of the robotic fish. Another camera recorded the swimming motion from the top view. Thus, the swimming speed and the “yaw” motion of the robotic could be calculated according to the coordinate behind the tank and the markers on the robotic fishes.

### A. Cruising With Fins

A series of experiments were conducted in the prepared tank, and the swimming speed and the stability of the robotic fish can be extracted by processing the sequence images from the cameras. Fig. 13(a) displays the swimming speed of the robotic fish in terms of various swimming parameters such as flapping frequency and amplitude of the caudal fins. It can be seen that swimming speed will be significantly improved with the opposite flapping of the caudal fins, which also validate the hypothesis that the opposite flapping caudal fins will bring a high swimming performance for it utilizes the characteristics of jet propulsion. Note that the highest swimming speed is 1.21 BL/s, which is relative high for the relative low power servo motors. However, despite the highest swimming speed occurs at 2.6 Hz with a 40° amplitude, which does not mean that the param-

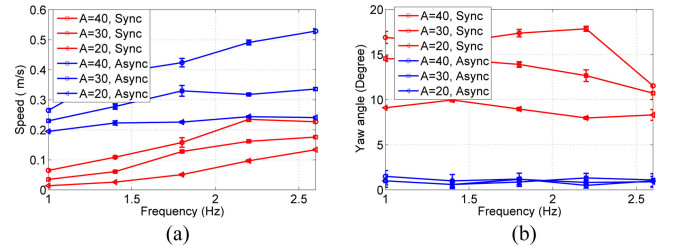


Fig. 13. Cruising with caudal fins. Blue lines denote swimming speed with opposite flapping caudal fins, while red lines denote swimming speed with synchronized flapping caudal fins.  $A$  denotes the amplitude of the caudal flapping: (a) swimming speed with caudal fins; and (b) “Yaw” angle of the robotic fish during swimming.

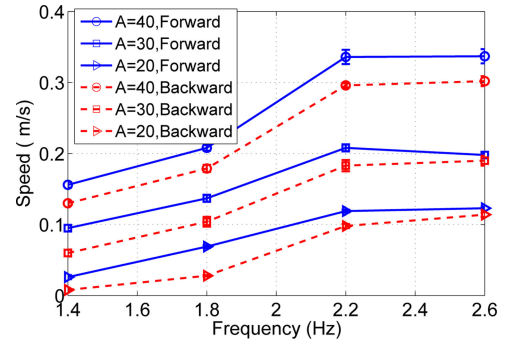


Fig. 14. Cruising with pectoral fins: (a) forward swimming speed with pectoral fins; and (b) backward swimming speed with pectoral fins.

eters are optimized for swimming performance. The reason is that the amplitude will decrease for a higher flapping frequency ( $> 2.6$  Hz) because of the power limitation of the motors. It can be expected that the swimming speed can be improved further by applying more powerful servo motors. Fig. 13(b) displays the instability of the robotic fish during swimming, that is the “yaw” motion during each flapping cycle. From the figure, it can be clearly concluded that the opposite flapping of the dual caudal fins possesses a much higher stability during swimming than that of synchronous flapping. The stability of the fish body during swimming is very important for the clear and stable images captured by the camera mounted on the robotic fish in environmental exploration or surveillance.

Fig. 14 displays the swimming speed of the robotic fish only propelled by two pectoral fins. The speed of the robotic fish by pectoral fins is relatively low compared to the speed by caudal fins. The meaning of cruising by pectoral fins is not the high speed, but the maneuverability in a complex environment. From the figure, we can also obtain that the pectoral fins could effectively propel the robotic fish to swim backward despite the speed is lower than that of forward swimming. The speed difference mainly arises from the drags generated in forward and backward swimming. Backward swimming is extremely useful for a robotic fish when it explores a narrow cave or a culvert underwater. For example, the robotic fish could escape from a dilemma by backward swimming, if it enters a blind alley during exploration.

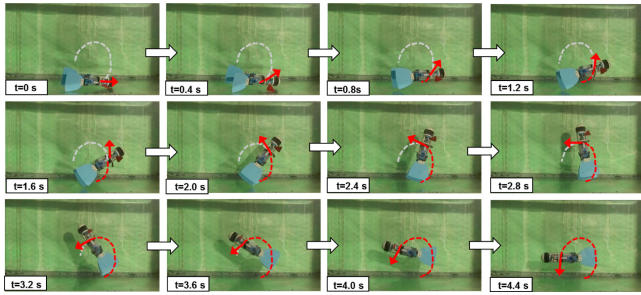


Fig. 15. Snapshot photos of the robotic fish during a back flip maneuver, red dashed line denotes trajectory that the robot has swum along, while white dashed line denotes the trajectory that the robot will swim along. Red arrow denoted the swimming direction of the robot. In the experiment,  $m_1=45$ ,  $m_4=-45$ ;  $\phi_{14} = \pi$ ; while  $R_{5,6}$  is set as a relative small constant, which means the caudal fins keep still.

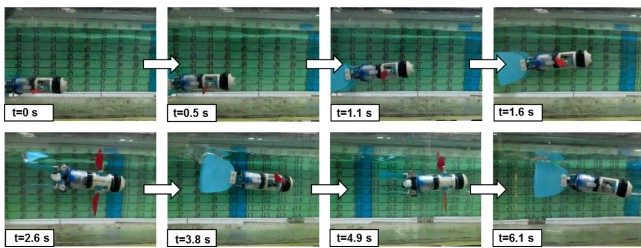


Fig. 16. Snapshot photos of the robotic fish during a rolling maneuver. In the experiment,  $m_{2,3}=45$ ;  $\phi_{14} = \pi$ ;  $R_{5,6} = 20$ , while  $R_{1,2,3,4}$  were set as a relative small constant to keep the pectoral fins still.

## B. Maneuvers

With coordinated motions of fins, the robotic fish can also realize plenty of maneuvers such as rising, sinking, rolling, and turning. With the pectoral fins propel forward and upward, the robotic fish can realize a rising motion. Moreover, the robotic fish can also implement a back flip motion with the pectoral continue propelling. The rotation radius of the back flip is about 20 cm, which is only one third of the body length. Fig. 15 displays the snapshot of the robotic fish executing a back flip. In the same way, the robotic can achieve a front flip motion with the pectoral fins propelling in another certain direction.

The robotic fish also can realize a rolling motion. In the rolling motion, the two pectoral fins keep still, locating at horizontal plane with a rolling angular difference between the fins. Fig. 16(a) displays the rolling motion of the robotic fish. The rolling speed of the fish in the figure is about 1.4 rad/s, which means the robotic fish could roll one cycle within 4.5 s. The rolling motion are also useful for adapting a complex environment. For example, the robotic fish could adjust its body posture to pass through a narrow aperture underwater.

The turning motion in the horizontal plane can be implemented in various methods: the fish could utilize its caudal fins to realize a turning motion. In the maneuver, the ratio between the instroke and the outstroke is about 1/3. However, the turning motion is not so smooth and effective compare to the multijoints BCF robotic fishes [4], [5], [36], [37]. The reason lies in that the multijoints BCF robotic fish can utilize their flexible body and caudal fin to generate a *C* shape turning, which decreases the turning radius

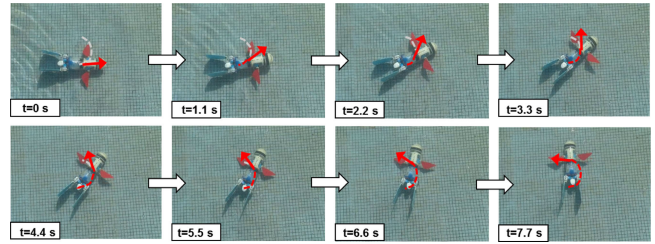


Fig. 17. Snapshot photos of the robotic fish during a turning maneuver with pectoral pins, red dashed line denotes trajectory that the robot has swum along, while white dashed line denotes the trajectory that the robot will swim along. Red arrow denoted the swimming direction of the robot. In the experiment,  $m_{1,4} = 0$ ;  $\phi_{14} = 0$ ;  $R_{1,2,3,4} = 20$ , while  $R_{5,6}$  were set as a relative small constant to keep the caudal fins still.

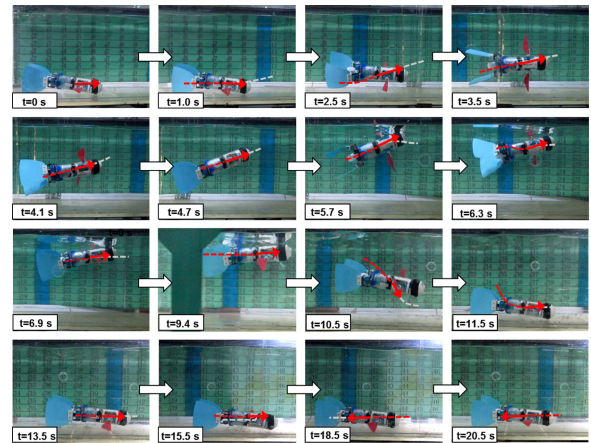


Fig. 18. Snapshot photos of the robotic fish switching various maneuvers, red dashed line denotes trajectory that the robot has swum along, while white dashed line denotes the trajectory that the robot will swim along. Red arrow denoted the swimming direction of the robot. The controlling CPG signal is shown in Fig. 11.

and increases turning speed. However, there is another method to achieve a turning motion for the developed robotic fish, which is analogous with the motions of the insects. That is, flapping two pectoral fins with different amplitudes and angles of attack to obtain a turning torque in horizontal plane [38]. Fig. 17 displays turning motion with the pectoral fins, the turning radius is about 10 cm, which is much smaller than that with the caudal fins.

## C. Autonomous Swimming

As described in Section IV, the robotic fish could achieve a smooth transition among its various maneuvers. Fig. 18 displays the experimental result corresponding to the CPG controlling in Fig. 11. The transitions among various maneuvers remains smooth, which is similar to the maneuvers performed by an animal.

With the feedback of three infrared sensors to the CPG network, the robotic fish could also implement an autonomous swimming. Fig. 19 displays the experimental result corresponding to the CPG controlling described in Section IV. In the experiment, the robotic fish first performed a steady swimming, then it rose for there exists an obstacle at its forward and downward direction. After that, the fish sank because the center and the

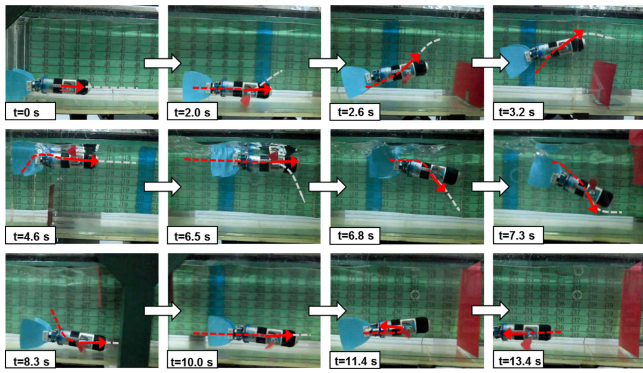


**Fig. 19.** Snapshot photos of the robotic fish during autonomous swimming, red dashed line denotes trajectory that the robot has swum along, while white dashed line denotes the trajectory that the robot will swim along. Red arrow denoted the swimming direction of the robot.

upward IR sensors returned obstacle signals. Finally, the robotic fish swam backward because the whole area before the head of the robotic fish is blocked. The experiment indicated that with some simple controlling strategies and sensors, the robotic fish could utilize its agility to perform an autonomous swimming. Due to the difficulty of the communications underwater between the robotic fish and the operators, autonomous swimming of the robotic fish provides a basis for its applications such as exploration in a complex underwater environment without manual operations.

#### D. Discussion

The experiments had demonstrated the agility of the robotic fish with the coordinated movement of various fins. The arrangement of dual caudal fins brings some merits to swimming performance. First, the highest swimming speed propelled by the opposite flapping of caudal fins is about 1.21 BL/s, which is much higher than that of synchronous flapping. It should be emphasized that the speed is achieved with low-power servo motors. The swimming speed could be improved with higher power motors. Second, the swimming stability of the robotic fish has been greatly enhanced. “Yaw” motion is a general problem in robotic fish, while the opposite flapping of caudal fins generates opposite lateral forces, which improves the swimming stability. Moreover, “roll” and “pitch” motion can also be controlled by the coordinated movement of the caudal fins and pectoral fins. The dual caudal fins mechanism was first applied in robotic fish in 2002 [39]. In their design, two ionic polymer-metal composite (IPMC) drivers were installed at the tail of a microbotic fish as the caudal fins. However, the merits of the caudal fins had not been explored for the driving limitation of IPMC. There have also been many developed fish-like prototypes with dual pectoral fins, including the MPF-like robotic fishes [7]–[9] and BCF-like robotic fishes [12], [40], [41]. In the MPF-like robotic fishes, the long base of dual pectoral fins usually requires more DOF, which increases the complexity of the structure. As for BCF-like robotic fishes, previous researches focused on the propulsion by the combined movements of body

and/or caudal fin [42]. Their pectoral fins usually performed only a rotation movement [12], [40], [41]. Lauder’s group has developed a state-of-art robotic pectoral fin that can perform various complex motions as those of BCF-like fishes [43]. However, the complex motions lead to complex and bulky driving modules, which hinders the equipment of the fin in a robotic fish. In our wing-like pectoral fins, the especially designed morphology analogical to that of insect wings endows the fins a longer leading edge than a traditional biomimetic pectoral fin, and the biomimetic motions of the wing-like fins deliver the robotic fish a strong maneuverability in vertical plane.

In this paper, we present the process of establishing a CPG network according to the requirement of the robotic fish. The CPG network is proved to be effective to control the maneuvers and cruising of the robot. Comparing to the typical CPG networks for biomimetic robots, there are some characteristics for the developed CPG. First, the developed CPG has clear descriptions for the key physical parameters such as frequency, amplitude, and phase difference, which is convenient to alter when the robot performs an emergent task or encounters a changing environment. Second, the govern equation of the oscillators is a first-order differential equation, which is simpler than that used in Salamander robot and Amphibot (a second-order differential equation) [22], [24] and decreases the computation load. In fact, only one microprocessor (PIC18F4550) accounted for obtaining the sensors information, calculating the result of the nonlinear oscillators, and outputting signals to six servo motors, which requires a simpler oscillation equation for the rhythm signal. Third, the evolving of the signal with various features is relatively rapid compared to the Hopf oscillator [8]. As shown in Fig. 6, the transition of phase difference can be accomplished in 1~2 oscillation cycle. In fact, the transitions of the amplitude and the frequency of controlling signal are also rapid. One limitation of the developed CPG is that the amplitude of the signals cannot be zero for the simplified differential equation. However, it can be overcome by outputting a small amplitude that can be ignored by the servo motors.

The novelty of this paper is the integrative biomimetic innovation in the design and controlling of robotic fish. We incorporated insect wings, dual caudal fins, and the CPG-based controlling method into one robotic fish to achieve a high maneuverability and a steady swimming. With two wing-like pectoral fins and their coordinated motions, vector thruster in vertical plane can be performed and agile pitching motions such as rising and sinking are easy to be accomplished. Moreover, the frontflip and backflip motions can also be obtained by continuous vectored thrust exerted in one direction, which is similar to the motions of dolphin robot despite the implementation is different [12]. Another remarkable characteristic is the robot can easily perform a rolling motion with two pectoral fins coordinated location, which is similar to the approach in [44]. With a gyroscope sensor equipped, the robot will be capable of adjusting and keeping its body with any certain rolling angle, which is meaningful for engineering applications. With the simple CPG network and infrared sensors, smooth transition between various maneuvers and autonomous swimming can be easily achieved.

## VI. CONCLUSION REMARKS

This paper is concerned with development of an integrative biomimetic robotic fish. By applying a pair of pectoral fins inspired by insect wings, the robotic fish achieved a strong maneuverability. By parallel arranging two caudal fins that surpasses nature, the robot could achieve a high locomotion performance and a more steady swimming. The detailed design of the robot is presented and the vectored thrusts exerted by various fins are introduced. A simple CPG network that satisfies the unique propulsion mechanisms of the robot and produces smooth and rapid transitions of the rhythm signals for plenty of maneuvers was developed. Swimming experiments on the robotic fish indicated the robot's maneuverability and validated the effectiveness of the CPG network. Autonomous swimming was also conducted with the feedback information of three IR sensors. The results demonstrated the agility and validity of the proposed synthesized biomimetic robot.

It is worth emphasizing that the purpose of the bioinspired fin was not to replicate fully the morphology of pectoral fins and caudal fins or not to perform exactly as those of the live fishes or insects. We aimed to develop a simple, durable, and low-cost robotic fish with a high performance, such as swimming speed, swimming stability, and plenty of maneuvers. In the design, the body of the robot was made of a rigid hollow cylinder, which means the body cannot transform with the change of the water pressure during rising or sinking. The controlling circuit and battery were sealed in the cylindrical can, which secures waterproof and improves the duration of the robot. The supportive framework for installing the pectoral fins were manufactured by 3D printing, which saves space and decreases the weight of the body. Combining with the agility of the robot, the developed robot shed a light on the engineering applications of underwater unmanned vehicles, such as exploration, surveillance, or observation on real fishes in a complex 3D underwater environment. Future work will include equipping more sensors on the robotic fish and conducting field tests to explore the swimming distance and to examine the feasibility of the robotic fish in applications.

## ACKNOWLEDGMENT

The authors would like to thank Mr. H. Huang and Mr. Y. Yang for their help in setting up the experimental platform and conducting the experiments.

## REFERENCES

- [1] M. S. Triantafyllou and G. S. Triantafyllou, "An efficient swimming machine," *Sci. Amer.*, vol. 272, no. 3, pp. 64–70, 1995.
- [2] C. M. Breder, "The locomotion of fishes," *Zoologica*, vol. 4, no. 2, pp. 159–296, 1926.
- [3] J. Yu, M. Tan, S. Wang, and E. Chen, "Development of a biomimetic robotic fish and its control algorithm," *IEEE Trans. Syst. Man, Cybern. B, Cybern.*, vol. 34, no. 4, pp. 1798–1810, Aug. 2004.
- [4] Q. Yan, Z. Han, S. Zhang, and J. Yang, "Parametric research of experiments on a carangiform robotic fish," *J. Bionic Eng.*, vol. 5, no. 3, pp. 95–101, 2008.
- [5] J. Liu and H. Hu, "Biological inspiration: From carangiform fish to multi-joint robotic fish," *J. Bionic Eng.*, vol. 7, no. 1, pp. 35–48, 2010.
- [6] T. Hu, L. Shen, L. Lin, and H. Xu, "Biological inspirations, kinematics modeling, mechanism design and experiments on an undulating robotic fin inspired by *Gymnarchus niloticus*," *Mech. Mach. Theory*, vol. 44, pp. 633–645, 2009.
- [7] Y. Cai, S. Bi, and L. Zheng, "Design and experiments of a robotic fish imitating cow-nosed ray," *J. Bionic Eng.*, vol. 7, no. 2, pp. 120–126, 2010.
- [8] C. Zhou and K. H. Low, "Design and locomotion control of a biomimetic underwater vehicle with fin propulsion," *IEEE/ASME Trans. Mechatronics*, vol. 17, no. 1, pp. 25–35, Feb. 2012.
- [9] Y. Cai, S. Bi, and L. Zhen, "Design optimization of a bionic fish with multi-joint fin rays," *Adv. Robot.*, vol. 26, pp. 177–196, 2012.
- [10] O. Curet, N. A. Patankar, G. V. Lauder, and M. A. MacIver, "Mechanical properties of a bio-inspired robotic knife-fish with an undulatory propulsor," *Bioinspir. Biomim.*, vol. 6, no. 2, pp. 026004-1–026004-9, 2012.
- [11] T. Hu, K. H. Low, L. Shen, and X. Xu, "Effective phase tracking for bio-inspired undulations of robotic fish models: A learning control approach," *IEEE/ASME Trans. Mechatronics*, vol. 19, no. 1, pp. 191–200, Feb. 2014.
- [12] J. Yu, Z. Su, M. Wang, M. Tan, and J. Zhang, "Control of yaw and pitch maneuvers of a multilink dolphin robot," *IEEE Trans. Robot.*, vol. 28, no. 2, pp. 318–329, Apr. 2012.
- [13] M. H. Dickinson, C. T. Farley, R. J. Full, M. A. R. Koehl, R. Kram, and S. Lehman, "How animals move: An integrative view," *Science*, vol. 288, pp. 100–106, Apr. 2000.
- [14] I. D. Nevelnb, E. Rothc, T. Mitchelld, J. Snyderb, M. MacIverb, E. Fortuneg, and N. Cowana, "Mutually opposing forces during locomotion can eliminate the tradeoff between maneuverability and stability shahin sefatia," *Proc. Nat. Acad. Sci.*, vol. 110, no. 47, pp. 18 798–18 803, 2013.
- [15] T. M. Kubow and R. J. Full, "The role of the mechanical system in control: A hypothesis of self-stabilization in hexapedal runners," *Phil. Trans. Roy. Soc. London Ser. B*, vol. 354, pp. 849–861, 1999.
- [16] J. Marden, "Maximum lift production during takeoff in flying animals," *J. Exp. Biol.*, vol. 130, pp. 235–238, 1987.
- [17] C. Ellington, C. Berg, A. Willmott, and A. Thomas, "Leading-edge vortices in insect flight," *Nature*, vol. 384, no. 19, pp. 626–630, 1996.
- [18] P. Zdunich, D. Bilyk, M. MacMaster, D. Loewen, J. DeLaurier, R. Kornbluh, T. Low, S. Stanford, and D. Holeman, "Development and testing of the mentor flapping-wing micro air vehicle," *J. Aircraft*, vol. 44, no. 5, pp. 1701–1711, 2007.
- [19] M. Keennon, K. Klingebiel, H. Won, and A. Andriukov, "Development of the nano hummingbird: A tailless flapping wing micro air vehicle," presented at the AIAA Aerosp. Sci. Meeting, Nashville, TN, USA, 2012, p. 1C24.
- [20] K. Ma, P. Chirarattananon, S. Fuller, and R. Wood, "Controlled flight of a biologically inspired, insect-scale robot," *Science*, vol. 24, no. 2, pp. 603–607, 2013.
- [21] A. H. Cohen, P. J. Holmes, and R. H. Rand, "The nature of the coupling between segmental oscillators of the lamprey spinal generator for locomotion: A mathematical model," *J. Math. Biol.*, vol. 13, no. 3, pp. 345–369, 1982.
- [22] A. Ijspeert, A. Crespi, D. Ryczko, and J.-M. Cabelguen, "From swimming to walking with a salamander robot driven by a spinal cord model," *Science*, vol. 315, no. 5817, pp. 1416–1420, 2007.
- [23] J. Yu, M. Wang, M. Tan, and J. Zhang, "Three-dimensional swimming," *IEEE Robot. Autom. Mag.*, vol. 18, no. 4, pp. 47–58, Dec. 2011.
- [24] J. Yu, R. Ding, Q. Yang, M. Tan, W. Wang, and J. Zhang, "On a bio-inspired amphibious robot capable of multimodal motion," *IEEE/ASME Trans. Mechatronics*, vol. 17, no. 5, pp. 847–856, Oct. 2012.
- [25] G. V. Lauder, P. Madden, R. Mittal, H. Dong, and M. Bozkurttas, "Locomotion with flexible propulsors: I. Experimental analysis of pectoral fin swimming in sunfish," *Bioinspir. Biomim.*, vol. 1, pp. s25–s34, 2006.
- [26] S. Zhang, B. Liu, L. Wang, Q. Yan, K. Low, and J. Yang, "Design and implementation of a lightweight bioinspired pectoral fin driven by SMA," *IEEE/ASME Trans. Mechatronics*, vol. 19, no. 6, pp. 1773–1785, Dec. 2014.
- [27] P. Webb, "Form and function in fish swimming," *Sci. Amer.*, vol. 251, pp. 58–68, 1984.
- [28] R. Clapham and H. Hu, "isplash-I: High performance swimming motion of a carangiform robotic fish with full-body coordination," in *Proc. IEEE Int. Conf. Robot. Autom.*, 2014, pp. 322–327.
- [29] M. Dickinson, F. Lehmann, and S. P. Sane1, "Wing rotation and the aerodynamic basis of insect flight," *Science*, vol. 284, pp. 1954–1960, 1999.
- [30] S. Fry, R. Sayaman, and M. Dickinson, "The aerodynamics of free-flight maneuvers in drosophila," *Science*, vol. 300, pp. 495–498, 2003.

- [31] R. Wood, "The first takeoff of a biologically inspired at-scale robotic insect," *IEEE Trans. Robot.*, vol. 24, no. 2, pp. 341–347, Apr. 2008.
- [32] A. J. Ijspeert, "Central pattern generators for locomotion in animals and robots: A review," *Neural Netw.*, vol. 21, no. 4, pp. 642–653, 2008.
- [33] J. Yu, M. Tan, J. Chen, and J. Zhang, "A survey on CPG-inspired control models and system implementation," *IEEE Trans. Neural Netw. Learn. Syst.*, vol. 25, no. 3, pp. 441–456, Mar. 2014.
- [34] A. Crespi, K. Karakasiliotis, A. Guignard, and A. Ijspeert, "Salamandra robotica II: An amphibious robot to study salamander-like swimming and walking gaits," *IEEE Trans. Robot.*, vol. 29, no. 2, pp. 308–320, Apr. 2013.
- [35] K. Seo, S.-J. Chung, and J.-J. E. Slotine, "CPG-based control of a turtle-like underwater vehicle," *Auton. Robot.*, vol. 28, no. 3, p. 247C269, 2010.
- [36] Z. Su, J. Yu, M. Tan, and K. Asaka, "Implementing flexible and fast turning maneuvers of a multijoint robotic fish," *IEEE/ASME Trans. Mechatronics*, vol. 19, no. 1, pp. 329–338, Feb. 2014.
- [37] J. Yu, L. Liu, L. Wang, M. Tan, and D. Xu, "Turning control of a multilink biomimetic robotic fish," *IEEE Trans. Robot.*, vol. 24, no. 1, pp. 201–206, Feb. 2008.
- [38] C. P. Ellington, "The novel aerodynamics of insect flight: Applications to micro-air vehicles," *J. Exp. Biol.*, vol. 202, pp. 3439–3448, 1999.
- [39] Z. Guo, T. Fukuda, and K. Asaka, "A new type of fish-like underwater microrobot," *IEEE/ASME Trans. Mechatronics*, vol. 8, no. 1, pp. 136–141, Mar. 2003.
- [40] W. Wang and G. Xie, "CPG-based locomotion controller design for a boxfish-like robot," *Int. J. Adv. Robot. Syst.*, vol. 11, pp. 87–1–87-11, 2014.
- [41] Y. Hu, J. Liang, and T. Wang, "Mechatronic design and locomotion control of a robotic thunniform swimmer for fast cruising," *Bioinspir. Biomim.*, vol. 10, pp. 026006-1–026006-17, 2015.
- [42] Y. Cha, J. Laut, P. Phamduy, and M. Porfiri, "Swimming robots have scaling laws, too," *IEEE/ASME Trans. Mechatronics*, vol. 21, no. 1, pp. 598–600, Feb. 2016.
- [43] J. Gottlieb, J. Tangorra, C. J. Esposito, and G. V. Lauder, "A biologically derived pectoral fin for yaw turn manoeuvres applied bionics and biomechanics," *Appl. Bionics Biomechan.*, vol. 7, pp. 41–55, 2010.
- [44] M. Nakashima, T. Tsubaki, and K. Ono, "Three-dimensional movement in water of the dolphin robot-control between two positions by roll and pitch combination," *J. Robot. Mechatronics*, vol. 33, no. 3, pp. 347–355, 2006.



**Shiwu Zhang** (M'12) received the B.S. degree in mechanical and electrical engineering, and the Ph.D. degree in precision instrumentation and precision machinery from the University of Science and Technology of China (USTC), Hefei, China, in 1997 and 2003, respectively.

He is currently an Associate Professor with the Department of Precision Machinery and Precision Instrumentation, USTC. His current research interests include smart materials and their applications in bioinspired robots, amphibious robot, and terradynamics.



**Yun Qian** received the B.E. degree in mechanical engineering from the University of Science and Science and Technology of China, Hefei, China, in 2014, where he is currently working toward the M.S. degree in the Department of Precision Machinery and Precision Instrumentation.

His research interests include biomimetic underwater robots and bioinspired control.



**Pan Liao** received the B.E. degree in mechanical engineering from the Southwest China University of Science and Science and Technology, Mianyang, China, in 2014. He is currently working toward the M.S. degree in the Department of Precision Machinery and Precision Instrumentation, University of Science and Technology of China, Hefei, China.

His research interests include biomimetic robots and microrobots.



**Fenghua Qin** received the B.S. degree in mechanical engineering and the Ph.D. degree in fluid mechanics from the University of Science and Technology of China (USTC), Hefei, China, in 1999 and 2005, respectively.

He is currently an Associate Professor with the Department of Modern Mechanics, USTC. His current research interests include self-propulsion motion of wing/fin, and applications and microfluidics.



**Jiming Yang** received the B.S. degree in engineering thermophysics and the Ph.D. degree in fluid mechanics from the University of Science and Technology of China (USTC), Hefei, China, in 1982 and 1992, respectively, and the Ph.D. degree in mechanical engineering from Tohoku University, Sendai, Japan, in 1995.

He is currently a Professor with the Department of Modern Mechanics, USTC. His current research interests include flapping wing motion and applications, high-speed aerodynamics and shock waves, and multiphase flow and measurements.